GEOCHEMISTRY

Rates of Carbon Cycling in a Coastal Wetland in Northwest Florida

Choi, Y., NHMFL/FSU, Geological Sciences
Wang, Y., NHMFL/FSU, Geological Sciences
Hsieh, Y.-P., FAMU, Wetland Ecology Program
Robinson, L., FAMU, Environmental Sciences Institute

Coastal wetlands are sensitive to global climate change and may play an important role in the global carbon cycle. However, the dynamics of carbon (C) cycling in coastal wetlands and its response to sea level change associated with global warming is still poorly understood. In this study, we collected soil samples, along a transect stretching from Low Marsh (the oldest part of the wetland) to High Marsh (the youngest part of the wetland) in a coastal wetland in north Florida for C and C isotopic analyses.

Changes in the radiocarbon and C content of soils between archived (1985) and present (1996 and 1997) samples were used, in conjunction with a mathematical model, to estimate the turnover times of soil C pools. Total carbon inventory in the study area is 31 kg C/m^2 in the Low Marsh (oldest part of wetland) and 18 kg C/m^2 in the High Marsh (youngest part of wetland). By examining the uptake of bomb ^{14}C in surfacial peat in archived and present cores, we estimated that the C turnover time in the surfacial peat (0-10 cm) is 20 years in the Low Marsh, and 4 years in the High Marsh. The carbon turnover time increases with depth in both Low Marsh and High Marsh. The current carbon accumulation rate in the surfacial peat (0-10 cm) is about 251 g C/m^2/yr in the Low Marsh, and about 127 g C/m^2/yr in the High Marsh. This suggests that the Low Marsh is sequestrating atmospheric carbon dioxide into soils, as soil organic matter, about twice as fast as High Marsh. The long-term C accumulation rate determined by examining the radioactive decay of radiocarbon as a function of depth is 18 g C/m^2/yr in the Low Marsh, and 45 g C/m^2/yr in the High Marsh.

These data suggest that the marshes in the area have been and continue to be a sink for atmospheric carbon dioxide. The much higher current rates of C accumulation in the marshes, in comparison with the long-term rates, may be caused by increased productivity due to global warming and/or increased global nitrogen deposition.

Using Nuclear Magnetic Resonance Spectroscopy to Study the Structure of Humic Acid

King, B.F., NHMFL
Gan, Z., NHMFL
Cross, T.A., NHMFL

Approximately 5% of most soils are comprised of organic matter. The organic fraction of soil (consisting primarily of humus, polysaccharides, lignins, and polypeptides) is very significant, for it determines soil productivity. The organic fraction of soil aids in the retention of nutrients via cation exchange, and in the adsorption of potentially toxic organic substances (e.g. pesticides, industrial wastes, etc.).

Humus is an amorphous brown-colored polymer formed by decomposed organic matter (e.g. dead plants and animals). It is subdivided into three categories depending upon its solubility in strong acids and bases. Humic acid is soluble only at pH values above 3; fulvic acid is soluble at all pH values; while, humin is insoluble.

The exact structure of humic acid is unknown and is dependent upon the source (which soil it is extracted from). Generally, humic acid consists of carbon, hydrogen, oxygen, and nitrogen; and, is comprised of various functional groups such as carbonyls, alcoholic and phenolic hydroxyls, carboxylates, amines, and amides. Humic acid has a very high cation exchange capacity; therefore, it is associated with the geochemical amassing of trace heavy metals—many of which are toxic to living things. Nevertheless, it is unclear at which sites the cation exchange processes are occurring.

It is suspected that much of this chemistry occurs at the carboxylate sites.

Several analytical techniques have been utilized to study humic acids. The application of nuclear magnetic resonance (NMR) spectroscopy to this problem is relatively new. The majority of these studies have been ^{13}C CP-MAS experiments. However, we are interested in solid-state ^{17}O NMR experiments. These experiments are being carried out on ^{17}O labeled Aldrich humic acid—to eventually understand the mechanism by which heavy metals and other pollutants interact with humic acids. The oxygen atoms, in the carboxyl groups of the humic acids, are often responsible for the cation exchange processes. Thus, it is of interest to study the oxygen atoms in humic acid. Nonetheless, ^{17}O NMR is not a popular technique due to the low natural abundance of oxygen (0.037%), its small magnetic moment, and its relatively large electric field gradient (resulting in lineshapes that are often broad and featureless). Furthermore, it is expensive to isotopically enrich oxygen.

Our ^{17}O experiments are being obtained on the 833 MHz Bruker spectrometer. A Hahn echo sequence is used to eliminate acoustic ringing from the probe. We use a recycle delay of 2 seconds, and acquired 80,000 scans (over a 4-day period). Our static spectrum yielded two very broad—overlapping signals—ranging from 0 ppm to 500 ppm (referenced to ^{17}O water at 0 ppm). The ^{17}O CSA values for carboxyl groups have not been published. However, the CSA values, for carbonyls that are a part of amide functional groups, can range from 500 ppm to 630 ppm. Thus, our results indicate that we have successfully labeled humic acid with ^{17}O, and have been able to detect a very insensitive nucleus utilizing a high magnetic field. These are very exciting results since there are no published studies of ^{17}O NMR done on humic acids. Additionally, there are very few published procedures for the labeling humic acids—most of these procedures refer to ^{13}C and ^{15}N labeling of synthetic humic acids. Currently, magic angle spinning experiments are being performed on this ^{17}O labeled humic acid, in order to minimize the line broadening. Spinning speeds up to 33 kHz are being used.

Acknowledgements: The authors wish to thank Dr. William Cooper and Dr. Gregory Choppin for all of their helpful discussions and advice about humic acids, and also for giving us humic acid samples. Furthermore, we are appreciative to Dr. Choppin for allowing us to use equipment in his laboratory. This work is supported by the NSF Research Training Grant.

Interactions of Mixed Uranium Oxides with Synthetic Groundwater and Humic Acid Using Batch Methods, Solubility Determinations, Experimentally and Calculated

Kurk, D., FSU, Chemistry
Choppin, G.R., FSU, Chemistry
Navratil, J.D., Clemson Univ., Chemistry
Salters, V.J.M., NHMFL/FSU, Geological Sciences

The possibility of container compromise within nuclear waste repositories makes it necessary to investigate potential interactions between the repository environment and the materials proposed for storage. Dissolution of the repository contents into the groundwater could result in migration of the radionuclides from the repository. This possible scenario necessitates the investigation of the waste materials solubility in groundwater.

The goal of this research was to determine the solubility of mixed uranium oxides in synthetic groundwater of the Snake River plain, under oxic and anoxic conditions at constant pH, in the presence and absence of humic acid. The values for the uranium solubility obtained experimentally and by calculations were compared.

The solubility experiment was performed for a total of 180 days. After a period of 104 days, all samples reached equilibrium. A plot of uranium concentration in solution versus time is given in the figure. In the absence of humics, the solubility of uranium was 0.098±0.002 g/L in anoxic conditions, and 0.114±0.002 g/L in oxic conditions. In the presence of humics, the solubility of uranium was 0.094±0.003 g/L in anoxic conditions, and 0.112±0.001 g/L in oxic conditions.

Uranium solubility calculations were performed using published data for uranium stability constants and solubility products. Results indicated that in the absence of humic acid, the oxic uranium solubility should be 0.117 g/L, which is very close to the experimental value. Calculations indicated that $CaUO_4$ controls the overall uranium solubility. Eh reached a stable value of +138±4 mV for anoxic samples, and +220±5 mV for oxic samples. The pH of oxic solutions between samplings increased to approximately 8.2, while for anoxic solutions it remained around 8.0. BET analysis showed that oxides had a surface area of 3.561±0.003 m^2/g. Sieving resulted in approximately 33% of the oxides being less than 170 mesh. XRD analysis indicated that a mixture of uranium oxides were present in the sample.

The results of these experiments imply the possibility of uranium oxides leaching into groundwater. Uranium entering the groundwater from a mixed oxide form is not a slow process on a geological time scale. The presence of humic acid at 1 ppm levels does not influence the uranium concentration as significantly as the presence of oxic conditions. Uranium solubility is less under anoxic conditions than under oxic conditions. The difference between oxic and anoxic solubility though does not imply that anoxic solubility should be ignored. The solubility calculations support the experimental findings of this research.

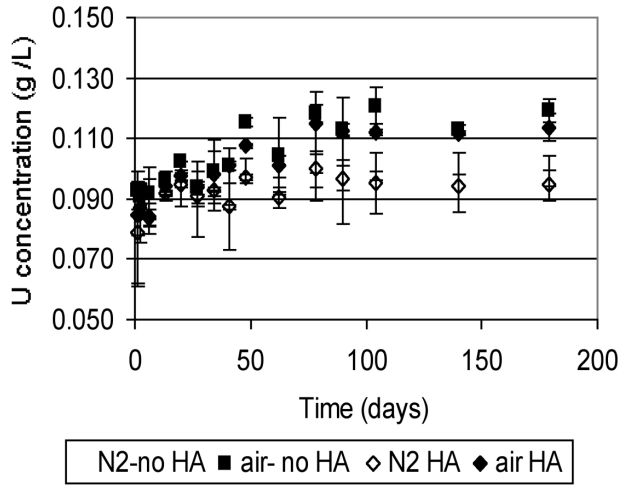

Figure 1. Uranium concentration in solution vs. time.

Isotope Dilution ICP-MS Analysis of Dissolved Iron in Seawater

Landing, W.M., FSU, Oceanography

A co-precipitation technique is being optimized to allow analysis of dissolved iron in seawater using isotope dilution ICP-MS. This continuing project utilizes the Geochemistry clean laboratory and the Finnigan Element ICP-MS at the NHMFL. The research is being conducted by Dr. Dave Kurk, a postdoctoral research assistant working with Prof. W.M. Landing in the Department of Oceanography at FSU.

This research supports an NSF-funded project to study the solubility and geochemical transformations of dissolved Fe in the surface ocean. Iron is now recognized as a bio-limiting, micro-nutrient element that controls phytoplankton productivity in vast regions of the surface ocean. Unfortunately, Fe(III) is very insoluble in seawater around pH 8; thus, there is a great need for accurate and sensitive analytical methods for measuring dissolved Fe at picomolar (10^{-12}) concentrations. High resolution magnetic sector ICP-MS is capable of resolving the major Fe isotope ^{56}Fe (91.7%) from the interference caused by argon oxide (approximately 57 amu); however, the seawater matrix (approx. 0.5 M NaCl plus 0.04 M $MgSO_4$) is too concentrated for accurate direct analysis. By co-precipitating the Fe (as the $Fe(OH)_{3(oxyhydroxide)}$ with $Mg(OH)_{2(s)}$) after the addition of ^{57}Fe yield tracer, the $^{56}Fe/^{57}Fe$ isotope ratio can be measured very accurately, allowing us to calculate the initial ^{56}Fe concentration with much better accuracy than any other analytical method currently available. Work to this point has emphasized the initial precipitation of the majority of the Ca^{2+} and Mg^{2+} (as their fluorides) using HF to further minimize the salt content of the Fe precipitate.

Acknowledgements: The author wishes to thank Dr. Vincent Salters for providing space in the NHMFL/Geochemistry clean laboratory, and for facilitating the ICPMS analysis.

Trace Metals in Aerosols by ICP-MS

Landing, W.M., FSU, Oceanography

The inter-relationships among trace elements in aerosol dust can be used to decipher the effects of anthropogenic vs. background (crustal dust) inputs to the atmosphere. Since aerosol deposition, either as dry deposition or as wet deposition in rainfall, represents the most important mechanism for the delivery of trace elements to the surface waters of the open ocean, we are interested in the chemistry of aerosols collected from remote marine locations.

Aerosol samples from Miami and Barbados, collected onto Whatman-41 cellulose filters, were totally digested using a combination of strong acids (HNO_3 and $HClO_4$) in the Geochemistry clean laboratory at the NHMFL and re-dissolved in 1% HNO_3 for analysis using the Finnigan Element ICP-MS in the Geochemistry group at the NHMFL.

The data are being used to compliment the interpretation of trace metal concentrations in a 2-year series of rain samples collected from Barbados. The project is the MS/Ph.D. project of Jerome J. Perry, a graduate student in the FSU Department of Oceanography. We are identifying anthropogenic vs. crustal dust aerosols using statistical correlations and factor analysis. By assuming some fractional rainfall and aerosol solubility in surface seawater (5 to 10%), we are able to estimate the deposition of a suite of trace elements to the open equatorial Atlantic. This is especially important for required micro-nutrient elements such as Mn, Fe, Co, and Zn. For Fe, a potentially bio-limiting, micro-nutrient element, the atmospheric deposition appears to exceed the supply of regenerated Fe from upwelling.[1]

Acknowledgements: The author wishes to thank Dr. Vincent Salters for providing the space and equipment in the NHMFL/Geochemistry clean laboratory for digesting the samples, and for facilitating the ICP-MS analysis.

[1] Landing, W.M., *et al.,* EOS Trans. Amer. Geophys. Union, **80**, 105 (2000).

Strontium Isotopes in the Mixing Zone of the Mississippi River: Implications for Ocean Budgets and Climate Change

Marcantonio, F., Tulane Univ., Geology

Earth scientists use Sr isotopes ratios as a tool with which to learn more about global climate change. Sr isotope investigations of sedimentary deposits have provided crucial information about chemical weathering of the continents, past temperature fluctuations, and global ocean budgets. Recently, researchers (Martin, *et al*., 1999; Stoll, *et al.*, 1999) have suggested that there may be differences in the cycling of Sr on glacial to interglacial timescales. Issues regarding its geochemistry must, therefore, be resolved. The conventional view is that strontium is a conservative element with a very long residence time (5 Ma; Broecker and Peng, 1982). Hence, it is assumed that dissolved Sr moves directly from rivers through estuaries to the ocean. In this view, there is little complexity in the biogeochemical cycle of strontium. Indeed, because of these assumptions most interpretations of the Sr isotope budget of the oceans, on which most climate models are based, rely on single analyses from several rivers throughout the world.

Sr isotope data gathered by Yingfeng Xu and Marcantonio on the NHMFL's Finnigan 262 thermal ionization mass spectrometer (Zindler and Salter laboratory) cast doubt on the simplistic view that Sr is conservative. Rather, a weak non-conservative behavior for this element is suggested. Indeed, Sr seems to be particle reactive and involved in hydrous Mn oxide particle dynamics. Such behavior has a direct bearing on estimates of the river flux of strontium to the oceans. Knowledge of this flux is crucial if we are to understand the strontium isotope record and the Sr/Ca record, and how each may be used to interpret global climate change.

Mercury Isotopic Evidence for r-Process Enrichment in the Allende Meteorite

Odom, A.L., NHMFL/FSU, Geosciences

The development of techniques to make high precision measurements of mercury isotope ratios has led to the recognition of significant variations in the isotopic composition of mercury due to mass fractionation, and has made it possible to define mass fractionation curves for terrestrial mercury. On plots of one isotope ratio versus another, a theoretical fractionation curve is the locus of the measured isotopic compositions of terrestrial mercury, provided the Earth formed with a single, well-mixed inventory of mercury. Fig. 1 is a previously obtained example of such a fractionation curve, and it demonstrates how well samples of both mercury ore minerals and industrially processed mercury conform.

Fig. 2 shows the same fractionation curve and less precise mercury isotope data obtained by previous workers on a number of different mercury reagents. Also included are the isotopic measurements of Nier and Schlutter (1986) for mercury from the carbonaceous chondrite Allende. The Allende data clearly depart from this terrestrial fractionation curve. Fractionation curves calculated for pairs of mercury isotope rations that do not include the isotope ^{204}Hg (e.g. curves of ^{198}Hg/^{200}Hg versus ^{199}Hg/^{202}Hg) fit both the terrestrial and Allende data.

The difference in terrestrial and Allende mercury is that, relative to terrestrial mercury, mercury in the Allende chondrite is enriched in mass 204. Mercury isotopes 198, 199, 200, 201, and 202 all reside along the valley of beta-stability and thus are products of low neutron-density, s-process nucleosynthesis, as initially defined by Burbidge, *et al. (*1957) and Cameron (1957). The neutron rich isotope 204 is the only mercury isotope produced only by the high neutron density r-processes that occur with the collapse of massive stars during super-nova events. The difference in the relative abundance of 204 Hg in the primitive meteorite Allende and in terrestrial samples is likely the result of incomplete mixing in the solar nebula during the time that lapsed between the injection of material from a super nova and the formation of the Earth and Allende.

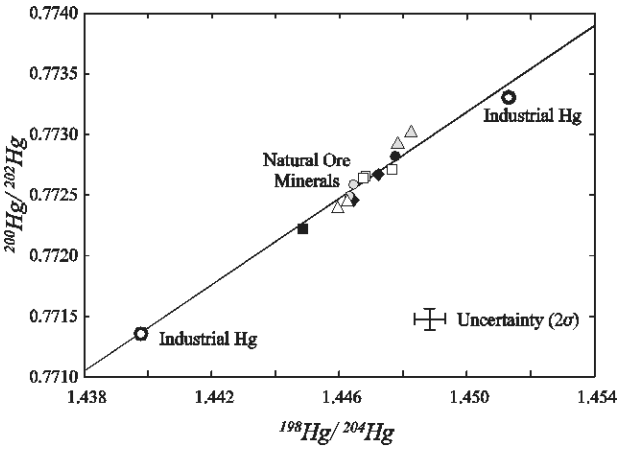

Figure 1. Plot of ^{198}Hg/^{204}Hg and ^{200}Hg/^{202}Hg isotope ratios of mercury in ore minerals and in two samples of industrially processed mercury (measurements made at the NHMFL). The line through the data is a calculated mass fractionation curve through the lower data point.

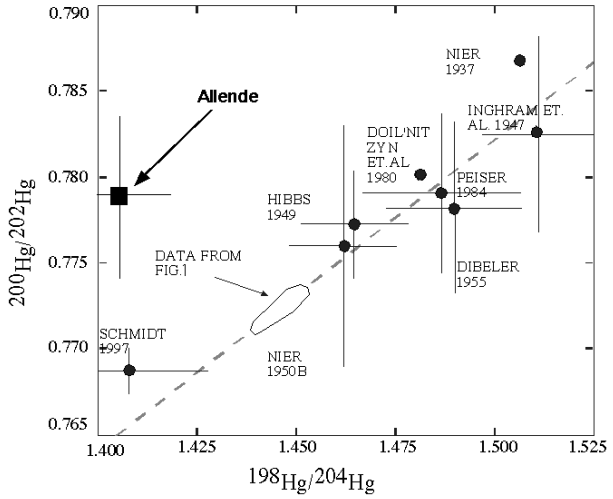

Figure 2. Dashed line is the mass fractionation line of Figure 1 and it includes all previously reported measurements of terrestrial mercury. Allende mercury is not described by the terrestrial fractionation line.

Metal Sources in Central Idaho Ore Deposits

Panneerselvam, K., Florida International Univ., Earth Sciences
Macfarlane, A., FIU, Earth Sciences
Salters, V., NHMFL

The Idaho-Montana region of the northwestern United States has been well-known for its mineral wealth since the early nineteenth century. World-class deposits like Butte, Montana and Coeur d'Alene, Idaho

occur here, together with many small to medium-sized deposits ranging from shale-hosted massive sulfides to granite and rhyolite-hosted epithermal Ag-Au deposits. Numerous ore-genesis studies around the world have invoked the participation of buried Paleozoic and Precambrian rocks as sources of ore metals, in addition to mantle-derived metal sources of various descriptions and the local host rocks.[7,12,6] Central Idaho presents an exceptional setting to evaluate these metal source issues because:

(1) The ores are hosted both by the Paleozoic metasedimentary host rock section and by intruding Cretaceous igneous rocks;
(2) A major Mesozoic sedimentary section is absent, simplifying the interpretation of isotope data;
(3) There is a large database of ore lead and sulfur isotope data available upon which to build;[4,5,3,9]
(4) Previous studies have identified large fossil hydrothermal systems in the area that have affected the exposed host rocks; [4,1,2,10] and
(5) Ore deposits occur over a wide area at varying distances from the margin of the Idaho Batholith, the dominant late-Cretaceous, early Tertiary magmatic event in the region.

Previous stable isotope and fluid inclusion studies indicated that the sediment-hosted ores were formed by meteoric water-dominated hydrothermal systems which incorporated sulfur from the Palezoic sedimentary host rocks. Radiogenic isotope studies concluded that Pb and other metal were derived from unidentified, deeper Precambrian rocks, not the Paleozoic host sequences. Many investigators[10,9] view the Late Cretaceous magmatism as a source of heat, but not as a significant source of ore components. This study is a comprehensive reevaluation of the metal sources for ores in this region, including an examination of the isotopic compositions of all of the major exposed crustal units and of dilute HCl and NaCl brine leachates of those units. These data are compared with new sulfur isotope data on ore minerals, new and published lead isotope data on ores, and published data for crustal xenoliths from the region to provide a new metal budget for central Idaho ore systems. The sediment-hosted systems are dominated by lead (and by inference other similarly transported metals) from the Paleozoic metasedimentary host sequences. Granite-hosted base and precious metal deposits contain metals derived from the host igneous rocks, for the most part. Thus, the upper crustal sequences in the region exert a strong control on the metal budgets of the ore forming systems, in contrast with what has been thought by earlier workers.

[1] Criss, R.E., *et al.,* Geol. Soc. Am. Bull., **94**, 640-663 (1983).
[2] Criss, R.E., *et al.,* Jour. Geophy. Res., **96**, 13,335-13, 356 (1991).
[3] Doe, B.R., *et al.,* USGS Bull., **2064** A-R. R.G. M1-M29 (1995).
[4] Hall, W.E., *et al.,* USGS Jour. of Res., **6**, 579-592, (1978).
[5] Howe, S.S., *et al.,* USGS Bull., **1658** A-S, 183-192 (1985).
[6] Lehuray, A.P., *et al.,* Econ. Geol., **82**, 1695-1709 (1987).
[7] Macfarlane, A.W., *et al.,* Intl. Geol. Rev., **36**, 645-677 (1994).
[8] Panneerselvam, K., *et al.,* Abstract. AGU Spring Meeting, Washington, D.C. (2000).
[9] Sanford, R.F., *et al.,* USGS Bull., **2064** A-R, N1-N24 (1995).
[10] Seal II, R.R., *et al.,* Econ. Geol., **87**, 271-287 (1992).
[11] Selvam, K.P., *et al.,* In Ninth Annual V.M. Goldschmidt Conference, p. 266., LPI Contribution No. 971, Lunar and Planetary Institute, Houston (1999).
[12] Tosdal, R.M*., et al.,* Sociedad Geologica del Peru, Volumen Jubilar Alberto Benavides, 311-326 (1995).

Parameterization of Trace Element Partitioning on the Mantle Solidus at Pressures up to 3.4 GPa

Salters, V.J.M., NHMFL, FSU, Geological Sciences
Longhi, J.E., Columbia Univ., Lamont Doherty Earth Observatory
Bizimis., M., Columbia Univ., Lamont Doherty Earth Observatory

We present new experimental partitioning data for a range of petrogenetically important elements up to pressures of 3.4 GPa, which is an extension of our previous study (Salters and Longhi, 1999). The experiments are designed to mimic melting beneath mid-ocean ridges. The available data indicates that the partition coefficients are pressure, temperature, and composition dependent. Therefore, if melt is extracted continuously during the adiabatic rise of mantle material, knowledge of partition behavior over the appropriate range of pressure, temperature and composition is required. For this purpose, we have parameterized the partitioning behavior of the REE,

Hf, Zr, U, and Th, based on a simple thermodynamic model. This parameterization shows that although it cannot be used for retrieving thermodynamic constants yet, the parameterization does yield a description of the partitioning behavior, which is useful for modeling decompression melting.

Our parameterization shows that on the peridotite solidus the partitioning of trace elements is strongly dependent on the Ca and Al-content of the clinopyroxene. However, REE are always incompatible in cpx on the peridotite solidus at pressures up to 3.4 GPa. For garnet, the data indicates that the heavy REE partition coefficients decrease with increasing pressure. One surprising result of the modeling of the partitioning is that, for both cpx and garnet, the substitution mechanism for the large tetravalent ions (U and Th) is different than for small ions (Hf and Zr). Our data indicates that Pb is more incompatible than Ce; and, in garnet, Ce and Pb have similar partition coefficients. Therefore, in order to explain the near-constant Ce/Pb ratios in MORB and OIB, a residual phase with high Pb partition coefficients is required. It is suggested that sulfides are the most likely phase that buffer the Pb content in the melt.

Fig. 1 and 2 show the trace element fractionations as a results of melting during adiabatic melting. This is the first model that adjust partition coefficients in response to changes in P, T, and X during melting. This more realistic model of trace element partitioning allows for a better estimation of degree and average depth of melting, as well as the modeling of the major element variations in conjunction trace element fractionations.

Clinopyroxene on the peridotite solidus is unable to fractionate U from Th to large enough extend that it can create the ^{230}Th excess in MORB. Garnet can fractionate U from Th effectively and is required for MORB genesis (see Fig. 1). Previous studies showed that the coupled Sm/Nd and Lu/Hf fractionation in MORB require residual garnet. The new partitioning parameterization of the REE and Hf is in agreement with these previous studies (see Fig. 2). Furthermore, the parametrization for clinopyroxene from this study results in estimates of partition coefficients that are similar to estimates using the Wood and Blundy (1997) model.

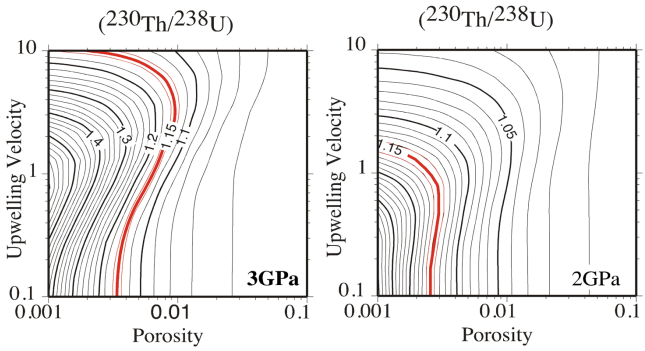

Figure 1. Contours of ^{230}Th-excesses for melts generated using the cpx and garnet parameterizations of this study for a range of upwelling velocities (0.1 to 1-cm/year) and a range of initial porosity (0.1% to 10%). Melting model used is that of Spiegelman and Elliott (Spiegelman and Elliott, 1993), using the web-based program Usercalc (Spiegelman, 2000). Lines in red are the 15% ^{230}Th-excess, which is the average excess of MORB. When melting starts at 3 GPa, 15% excess can be created at porosities that are up to 1% and matrix upwelling velocities of between 2 and 7 cm/year. In contrast, if melting starts at 2 GPa, i.e., no garnet present, 15% excess can only be created at porosities less than 0.3% and upwelling velocities of less than 2 cm/year.

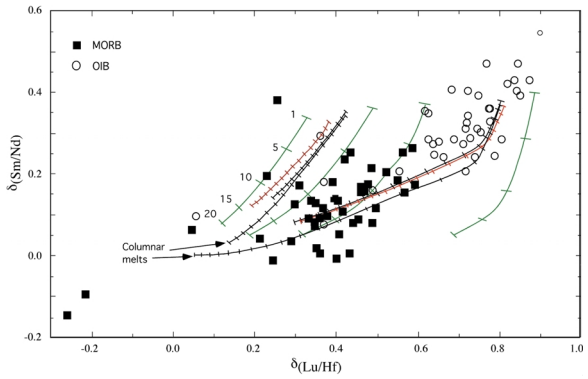

Figure 2. $\delta_{(Lu/Hf)}$ versus $\delta_{(Sm/Nd)}$ diagram with various melting curves for the different trace element parameterization. Melting curves are the aggregated melts from the complete melting regime. Except for where noted, melting curves are for triangular melting regime. Green curves are old models (Salters and Hart, 1989), numbers at tick marks on left most green curve is extend of melting (in percent) for a peridotite unit that has undergone the largest degree of melting in the melting regime (i.e. ascended directly under a ridge). Black curves use the trace element parameterization presented in this study combined with the Longhi model for fractional melting at decreasing pressure. Tick marks are at 1% melt increments of the peridotite unit that has undergone the largest degree of melting in the melting regime. Red curves are the same as the black curves, but Wood and Blundy parameterization for cpx partitioning. The experimental database for both cpx partitioning models was the same.

Metal Speciation by Capillary Electrophoresis Inductively Coupled Plasma Mass Spectrometry (CE-ICP-MS)

Sonke, J.E., NHMFL
Salters, V.J.M., NHMFL

We report on capabilities for elemental speciation studies through coupling of capillary electrophoresis (CE) to a high resolution magnetic sector ICP-MS. The superior multi-element detection capability of ICP-MS and the separation potential of CE provide the basis for determining elemental speciation in aqueous solutions.

The key to coupling both techniques is the interface, which closes the electrical CE circuit and optimizes mass transport into the ICP-MS. Full control of the electrolyte flow in the CE capillary allows for optimal tuning of a specific separation experiment. At the cost of resolution, rapid analyses times (3 min) make possible kinetic studies of complexation reactions. Longer analyses times (30 min) may facilitate the high resolution necessary for metal-humic separations.

We used CE-ICP-MS to study equilibrium speciation and kinetics of Cu-EDTA binding involving both ligand (EDTA, humics) and metal (Cu, Zn) competition at micro molar levels. Fig. 1 shows the Cu-speciation as a function of time after adding Cu to a Zn saturated solution of EDTA and humic acids. Results indicate retardation of Cu-EDTA binding on a ~20-minute time scale. Cu-humic binding is instantaneous, suggesting different Zu and Zn binding sites on the humic macromolecule.

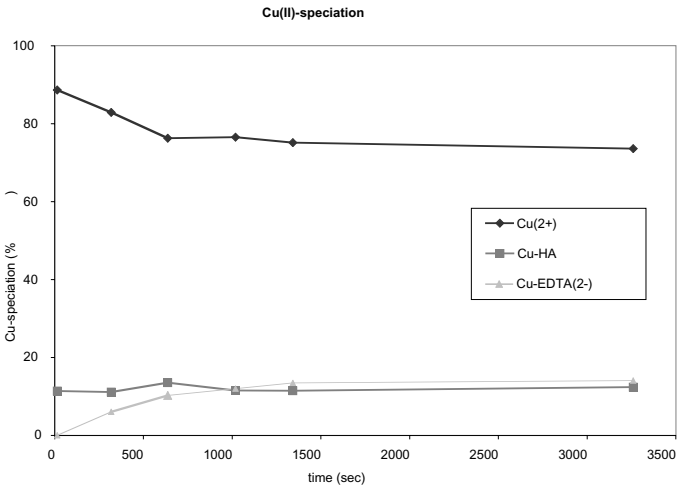

Figure 1. Changes in Cu-speciation as a function of time. Addition of Cu to a Zn saturated EDTA+humics solution causes instantaneous formation of Cu-humic complexes while Cu-EDTA formation is retarded by Zn release.

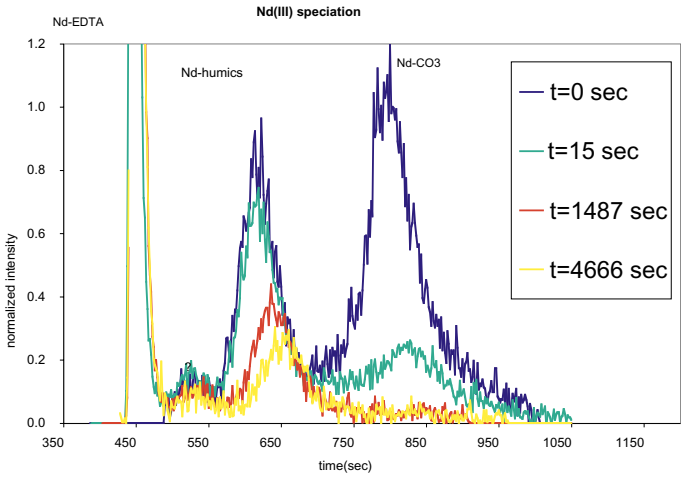

Figure 2. Stacked electropherograms of Nd speciation showing changes after adding EDTA to an equilibrated Nd-humics solution (pH 8.1). Nd release from CO_3 is rapid, whereas release from humics is slow.

Similar results were obtained when perturbing an equilibrium speciation of Nd(III)-humics at pH 8.1, by adding EDTA to solution. Fig. 2 shows the stacked electropherograms at different time intervals after adding EDTA. Nd rapidly converts from the CO_3 complex to the EDTA complex, however, Nd release from the humic complexes is slower. Equilibrium and kinetic studies of Nd speciation may give insight into actinide behavior under similar conditions.

Kinzer, J.A., *et al.,* Analytical Chemistry, **68**, 3250-3257 (1996).

Geochemistry of Volcanic Rocks from Small and Large Eruptive Centers in the Villarrica Region, Chile

Sun, M., Florida International Univ., Earth Sciences
Hickey-Vargas, R., FIU, Earth Sciences

One of the major questions in understanding the origin of magma in subduction zones is how chemical components are transferred from subducted sediments and oceanic crust, and incorporated into

the magmas that are ultimately erupted on the surface. The objective of this NSF-supported project is to evaluate possible transfer processes by examining the geochemistry of a cluster of contemporateous subduction-related volcanic centers that erupt magmas of markedly different trace element and isotopic character.

Sr, Nd and Pb isotope ratios for 18 rock samples were measured on the Finnegan mass-spectrometer in the Geochemistry Section of the NHMFL. Results of these measurements are combined with data obtained elsewhere, including multiple trace element analyses by ICPMS and ICPES, analyses of 10-Be by accelerator mass spectrometry, and U-series isotopes by alpha spectrometry.

Modeling of the results suggests that magmas from small eruptive centers clustered around a large stratovolcano incorporated a smaller amount of slab-derived hydrous fluid and fluid-soluble elements than magmas erupted at the central large edifice. Interestingly, the fluid incorporated by magmas erupted at the small centers has a higher proportion of elements derived from sediment relative to elements derived from altered basaltic crust. These fluids are probably formed at least in part by sediment melting. The overall result is that extraction of elements from the subducted lithosphere over small distance scales (20 km) may take the form of a chemically zoned region of hydrous fluids and melts leaving the subducted crust and causing production of a chemically zoned column of magma rising through the mantle wedge.

Carbon Isotopic Evidence for the Source and Fate of Dissolved Organic Matter in the Florida Everglades

Wang, Y., NHMFL/FSU, Geological Sciences
Hsieh, Y.-P., FAMU, Wetland Ecology Program
Landing, W.M., FSU, Oceanography
Choi, Y.H., NHMFL/FSU, Geological Sciences
Salters, V., NHMFL/FSU, Geological Sciences

The natural carbon isotopic ratios of dissolved organic compounds (DOC) reflect the sources and fates of DOC in an ecosystem. In the surface waters in the Florida Everglades, DOC can come from the historic peat deposits, "modern" wetland vegetation, and sugarcane (the dominant agricultural crop in the Everglades Agricultural Area). Stable carbon isotope analyses of DOC, plants, and soils collected from the northern Everglades indicate that less than about 23% of the DOC was derived from sugarcane, and the amount of DOC from sugarcane was greater under dry conditions. Water samples containing higher proportions of sugarcane-derived DOC also had higher amounts of soluble reactive phosphate and lower amounts of DOC and DOP (dissolved organic phosphorus). Most of the DOC (>50%) in the northern Everglades were in the low molecular weight (<1000 Dalton) fraction. The relative amount of high molecular weight (>1000 Dalton) DOC was higher in the wet period than in the dry period.

Radiocarbon ages of DOC in the northern Everglades ranged from ">modern" to about 2400 years B.P., indicating that DOC was derived from both historic peat deposits and modern vegetation. The very old radiocarbon ages of DOC in canal discharges indicate that the historic peat deposits in the Everglades Agricultural Area were a predominant source of DOC in the inflow waters to the Everglades Water Conservation Areas and the Everglades Nutrient Removal Project. In contrast, the DOC in the pristine area in the northern Everglades had "young" radiocarbon signatures and was primarily derived from recent photosynthate. At each site, the high molecular weight DOC (>1000 Dalton) had older radiocarbon ages than the low molecular weight DOC (<1000 Dalton), and therefore contained a greater fraction of DOC derived from the historic peat deposits. It appears that at least some of the old DOC from the historic peat deposits were decomposed by microbes during their residence in the surface water system in the northern Everglades, and the low molecular weight DOC was more microbially labile than the high molecular weight DOC. Our analysis suggests that accelerated decomposition of organic matter in the historic peat deposits (due to land-use change) could provide a significant source of DOC and nutrients for aquatic organisms in the northern Everglades.

Our data also suggest that the radiocarbon signature of DOC could be used as a sensitive indicator of the overall effectiveness of a wetland restoration project.

Radiation Response of E'_1 Centers in Quartz up to Gigarad Doses

Xie, J., NHMFL/FSU, Geosciences
Odom, A.L., NHMFL/FSU, Geosciences

The dosimetric properties of quartz have been used in determining the ages of certain geologic and archeologic materials. Although, it is now recognized that certain EPR centers associated with Schottkey-Frenkle pairs can continue to accumulate over time scales of 10^8 years. Reliable "ages" can presently only be obtained on specimens less than about 10^6 years old. This is because at moderate dose levels, EPR centers whose precursors are extrinsic, crystal defects reach a maximum (existing traps become filled), and those associated with intrinsic Schottkey-Frenkle pairs have a simple, nearly linear radiation sensitivity only at low doses.

To study the high dose level response of the E'_1 center, (a hole trapped at an oxygen vacancy), samples of volcanic quartz were subjected to incremental gamma radiation doses up to $10x10^9$ rads, and the increase in centers were monitored by EPR spectrometry. The data obtained are well fitted by the following equation:

$$\mathbf{I = I_N + (I_M - I_N)(1-exp(-c \times dose))+\kappa \times dose},$$

where **I** is the intensity of an observed center, $\mathbf{I_N}$ the natural intensity prior to artificial radiation, $\mathbf{I_M}$ is the maximum EPR intensity induced by artificial radiation (when all traps are filled), **c** is the sensitivity constant (in the exponential part), κ is the sensitivity constant (in the linear part), and dose is the radiation dose.

The exponential part plays an important role in low dose radiation in which the formation of centers is implemented through existing precursors (vacancies). Since the number of traps is limited, the probability of electrons being trapped decreases, as more traps became filled. The linear part plays the major role in high dose radiation (such as the gigarad range), in which the formation of centers is implemented through a radiolytic process in which new vacancies are formed, and, at the same time, trap holes to form the E'_1 centers. The fitting analysis indicates that atomic displacement occurs in high dose of gamma radiation ($10x10^9$ rads).

The sensitivity constants are unique for each specimen of quartz studied. The radiation response of the quartz specimen is influenced by the number and stabilities of competing hole and electron centers, and the constants must be determined by fitting data obtained from artificial radiation experiments. With these values, it is then possible to extract the natural dose a sample had received, and from that plus a knowledge of the ambient radiation background, its age.

Another oxygen-vacancy related center could be observed at high microwave power (where E_1' saturates) in most of the quartz samples. In powder spectra, this signal is centered at g=2.0077. The intensity of the EPR signal of this center can also be described by the equation above.

Acknowledgements: This work has been funded by the National Science Foundation and the Atomic Energy Control Board of Canada.